frontiers in Oncology

ORIGINAL RESEARCH
published: 28 May 2019
doi: 10.3389/fonc.2019.00439

Prognostic Value of the Neo-Immunoscore in Renal Cell Carcinoma

Congfang Guo[1,2,3,4,5,6†], *Hua Zhao*[1,2,3,4,5†], *Yu Wang*[6], *Shuai Bai*[7], *Zizhong Yang*[8], *Feng Wei*[1,2,3,4,5*†] *and Xiubao Ren*[1,2,3,4,5*†]

[1] Department of Immunology, Tianjin Medical University Cancer Institute and Hospital, Tianjin, China, [2] National Clinical Research Center for Cancer, Tianjin, China, [3] Key Laboratory of Cancer Prevention and Therapy, Tianjin, China, [4] Tianjin's Clinical Research Center for Cancer, Tianjin, China, [5] Key Laboratory of Cancer Immunology and Biotherapy, Tianjin, China, [6] Department of Emergency, Tianjin First Center Hospital, Tianjin, China, [7] Department of Gastrointestinal Cancer Biology, Tianjin Medical University Cancer Institute and Hospital, Tianjin, China, [8] Nankai University School of Medicine, Tianjin, China

Objective: This study evaluated the prognostic value of the newly-built Immunoscore (neo-Immunoscore) in patients with renal cell carcinoma (RCC).

Methods: Eighty-two patients with RCC were enrolled in this study. Their 3- and 5-year survival rates and overall survival (OS) were evaluated. The clinicopathologic data of the 82 patients were collected and analyzed. CD3, CD4, CD8, CD45RO, Foxp3, tumor necrosis factor receptor type II (TNFR2), programmed death ligand-1 (PD-L1), CD68, programmed death-1 (PD-1), cytokeratin (CK), and indoleamine 2,3-dioxygenase (IDO) were separated into two panels and stained using multiplex fluorescent immunohistochemistry methods. An immunologic prediction model of RCC patients, the neo-Immunoscore (neo-IS), was constructed using a Cox regression model. For the prognostic prediction of RCC, the neo-IS with the immunoscore (IS) proposed by the Society for Immunotherapy of Cancer (SITC) were compared by receiver operator characteristic (ROC) curve analysis. Survivals between the neo-IS_{low} and neo-IS_{high} groups were analyzed using the Kaplan–Meier method. Multivariate Cox regression survival analysis was applied to analyze independent indicators.

Results: The Cox regression model allowed the establishment of a neo-IS based on three features: $CD3^{+}_{CT}$, $CD4^{+}Foxp3^{+}CD45RO^{+}_{CT}$, and $CD8^{+}PD\text{-}1^{+}_{IM}$. Compared to that of the IS proposed by the SITC, the neo-IS obtained a better prediction. The 3- and 5-year survival rates in neo-IS_{high} RCC patients were significantly higher than those in neo-IS_{low} RCC patients (94.7 vs. 77.4%, $P = 0.035$ and 94.7 vs. 64.5%, $P = 0.002$, respectively). The OS in the neo-IS_{low} group was significantly shorter than that in the neo-IS_{high} group (73 vs. 97 months, $P = 0.000$). In comparisons of the neo-IS with clinical pathological factors, we found that the risk stratification and neo-IS were independent factors for the prognosis of patients with RCC. Moreover, the OS rate of neo-IS_{high} RCC patients with low- and intermediate- risk was higher than that of neo-IS_{low} patients.

Conclusion: The newly-constructed IS model more precisely predicted the survival of patients with RCC and may supplement the prognostic value of risk stratification.

Keywords: renal carcinoma, multiplex fluorescent immunohistochemistry, neo-immunoscore, risk stratification, prognosis

OPEN ACCESS

Edited by:
Fabio Grizzi,
Humanitas Research Hospital, Italy

Reviewed by:
Retnagowri Rajandram,
University of Malaya, Malaysia
Roberto Sabbatini,
Azienda Ospedaliero-Universitaria di Modena, Italy

***Correspondence:**
Feng Wei
iwhiffle@outlook.com
Xiubao Ren
renxiubao@tjmuch.com

†These authors have contributed equally to this work

Specialty section:
This article was submitted to Genitourinary Oncology, a section of the journal Frontiers in Oncology

Received: *21 February 2019*
Accepted: *08 May 2019*
Published: *28 May 2019*

Citation:
Guo C, Zhao H, Wang Y, Bai S, Yang Z, Wei F and Ren X (2019) Prognostic Value of the Neo-Immunoscore in Renal Cell Carcinoma. Front. Oncol. 9:439. doi: 10.3389/fonc.2019.00439

INTRODUCTION

As one of the major urological cancers, renal cell carcinoma (RCC), which derives from renal tubular epithelial cells, constitutes ∼3.8% of all cancers (1). RCC develops in about 295,000 people worldwide every year, with approximately 134,000 deaths due to RCC (2). The 5-year survival for kidney cancer is 74.5%; while 65.2% of kidney cancers are diagnosed at the local stage, the 5-year survival for localized kidney cancer is 92.6% (3). Even when curative surgery is performed for localized RCC patients, 20–30% experience recurrence or metastasis (1).

At present, the conventional prognostic prediction for RCC after radical nephrectomy is based on the American Joint Committee on Cancers (AJCC) pathological tumor-node-metastasis (TNM) classification system. Other pathological and clinical variables, including Fuhrman nuclear grade, necrosis, and Eastern Cooperative Oncology Group (ECOG) score have been implemented to improve the prognostication. Combining these tools together, the University of California Los Angeles Integrated Staging System (UISS) risk stratification provides a prognostic prediction for localized RCC (4). However, its predictive accuracy is still not comprehensive because it fails to incorporate the host immune response, which constitutes the major component of the defense system during tumor progression. In 2007, "immune contexture" including subtypes ($CD3^+CD8^+$, $CD3^+CD45RO^+$), functional orientation (Th1 cell-associated factors, cytotoxic factors, chemokines, cytokines, and adhesion molecules), density and location [tumor center [CT], invasive margin [IM] and the quality of tertiary lymphoid structures [TLS]] of immune infiltrating cells, were reviewed to show the important role of the immune system and a superior prognostic factor in cancers (5). Most studies have shown that high densities of $CD3^+$ T cells, $CD8^+$ cytotoxic T cells, $CD45RO^+$ memory T cells, and granzyme B (GZMB) in both the CT and the IM are related to an improved overall survival (OS) (6). Because of the complexity of the immune contexture, the immunoscore (IS), which derived from the immune contexture and based on immune cell density, has been confirmed as a simple immune classification and a clinically useful prognostic marker in cancers. Due to the high background staining and loss of antigenicity of CD45RO and GZMB, Galon and other researchers proposed the use of two easy membrane stains, CD3 and CD8, both in CT and IM in the IS system proposed by the Society for Immunotherapy of Cancer (SITC) to initiate a task force to validate its use in standard clinical practice as a new approach for the classification of tumors (7). Several studies on the IS have focused on gastrointestinal tumors (8), as well as other cancers, such as lung cancer, liver cancer, and head and neck carcinoma (9, 10). However, few studies have assessed the prognostic factor of the IS in RCC; thus, our study explored the significance of the IS to predict the prognosis of patients with RCC.

The immunosuppressive microenvironment is well-known to play pivotal roles in tumor progression. $CD4^+Foxp3^+$ regulatory T cells (Tregs) are prototypical immunosuppressive cells that dampen excessive immune responses and maintain homeostasis of the immune system. Mechanisms of Treg-mediated suppression include secretion of immunosuppressive cytokines, cell-contact-dependent suppression and functional modification or killing of APC (11). RCC patients with increased Tregs had a poor clinical outcome (12). Subset of Treg expressing TNFR2 shows increased suppressive function relative to those that did not express tumor necrosis factor receptor type II (TNFR2) (13). $CD45RO^+$ Treg (Memory Treg) cells have high immunosuppressive capacity and persist in the absence of antigen or low-level intermittent antigen exposure. Study of memory Treg cells in human has mainly focused on peripheral blood cells. It is important to study human memory Treg cells in tissues (14). On the other hand, macrophages are an important immune population. It can be subdivided into M1 and M2. M1 macrophages secrete pro-inflammatory cytokines and have a pro-inflammatory role. M2 macrophages have an anti-inflammatory role and favor tumor progression. Tumor associated macrophages (TAMs) are considered to be M2 macrophages according to widely accepted classification of macrophage. Increased infiltration of $CD68^+$ TAMs in tumor tissues was correlated with recurrence in patients with RCC (15).

Tumor-induced immune suppression which is mediated by the programmed death-1 (PD-1) and its ligand, programmed death ligand 1 (PD-L1) make cancer cells evade the host immunity. PD-1, which is induced on effector T-cell, limits T-cell function in various peripheral tissues and conduce to tumor progression. Interaction of PD-1 with PD-L1 provides an immune escape mechanism for tumor cells by turning off cytotoxic T cells (16). In addition, indoleamine 2,3-dioxygenase (IDO), as a rate-limiting enzyme within a tryptophan-depleted microenvironment, represents some metabolism characteristics of RCC (17). However, few reports have included these markers in the IS system.

We incorporated these immunosuppressive factors into our newly-built IS model. In the present study, we incorporated TAM, Treg and its co-inhibitory molecules, CD8 or CD68 coexpressing PD-1 or IDO, CD3 coexpressing PD-L1 to build a novel immune feature-based score to predict the OS of RCC patients after nephrectomy and compared this new model to the IS proposed by the SITC.

Cytokeratin is a key tumor marker of epithelium origin; therefore, we analyzed its prognostic value for RCC and used cytokeratin to determine the expression of IDO in tumor or mesenchymal cells (18). As clear-cell renal cell carcinoma (ccRCC) is the most commonly encountered morphotype of RCC (19), we selected ccRCC patients to participate in our study.

METHODS

Patients and Tissue Samples

Formalin-fixed paraffin-embedded specimens from tumor tissue of 82 RCC patients were included in this study and analyzed by multiplex fluorescent immunohistochemistry. The 82 patients were primary, biopsy-confirmed between January 2009 and January 2011 at Tianjin Medical University Cancer Institute and Hospital, Tianjin, China. These patients did not receive targeted therapy or immunotherapy before surgery. The study

was approved by the Ethics Committee of Tianjin Cancer Institute and Hospital. Each patient gave written informed consent. According to the American Joint Committee on Cancer (AJCC)/Union for International Cancer Control (UICC) tumor–node–metastasis (TNM) staging system (4), the patients were classified as RCC subtypes I–II and III–IV. Based on the University of California Los Angeles Integrated Staging System (UISS) (4), the patients were categorized as low, intermediate, or high-risk. Neutrophil count, lymphocyte count, hemoglobin, platelet count, urea nitrogen, lactic dehydrogenase (LDH), beta-2 microglobulin (β2-MG) were obtained from peripheral blood samples before operation. NLR was calculated with neutrophil-to-lymphocyte ratio. The distributions of the patient demographic and clinical characteristics are listed in **Table 1**.

Multiplex Fluorescent Immunohistochemistry and Multispectral Imaging

We selected 11 markers for multiplex fluorescent immunohistochemistry (IHC) staining to detect pan T cells (CD3), helper T cells (CD4), memory T cells (CD45RO), forkhead box P3 (Foxp3), TNFR2, and programmed death ligand-1 (PD-L1) by seven-color IHC and cytotoxic T cells (CD8), macrophages (CD68), programmed death-1 (PD-1), cytokeratin (CK), and indoleamine 2,3-dioxygenase (IDO) for six-color IHC. We analyzed the expression levels of single-stained cells, double-stained cells ($CD3^+PD\text{-}L1^+$, $CD8^+PD\text{-}1^+$, $CD68^+PD\text{-}1^+$, $CD8^+IDO^+$, $CD68^+IDO^+$, and $CD4^+FoxP3^+$), and triple-stained cells ($CD4^+Foxp3^+CD45RO^+$ and $CD4^+Foxp3^+TNFR2^+$) in the CT and IM of RCC specimen slides.

Multiplex fluorescent staining was obtained using Opal-7-Color Manual IHC Kit (NEL81001KT, PerkinElmer). The slides were deparaffinized in xylene and rehydrated in ethanol. Antigen retrieval was performed in AR 9.0 Buffer with microwave treatment (MWT). The tissue sections were covered with PerkinElmer Antibody Diluent blocking buffer and incubated for 10 min at room temperature. Primary antibodies for PD-L1 (66248-1-Ig Proteintech, 1:2000) were incubated in a refrigerator at 4°C overnight. The following day, the slides were incubated in Polymer HRP Ms+Rb for 10 min at room temperature. Visualization of PD-L1 was amplificated using Opal 520 TSA Plus (1:100). Then, the slides were antigen retrieved in AR 6.0 buffer with heated MWT. The preceding steps, including blocking, primary antibody incubation, introduction of HRP, signal amplification, and antibody stripping via microwave treatment were repeated until all targets of interest, including CD45RO (55618S CST, 1:2000), Foxp3 (MAB8214 R&D, 1:500), CD4 (ab133616, 1:500), TNFR2 (ab109322, 1:400), and CD3 (MA5-14524 Invitrogen, 1:300) were detected using a corresponding Opal fluorophore (Opal 540, Opal 570, Opal620, Opal650, or Opal690). The cell nuclei were finally stained with 4′,6-diamidino-2-phenylindole solution and the slides were cover-slipped with mounting medium. PD-1 (ab137132, 1:800), CD68 (ZM-0464, ZSGB-BIO, 1:200), CD8 (ab4055, 1:400), IDO (ab55305, 1:800), and CK (ZM-0069, ZSGB-BIO, 1:500) were

TABLE 1 | Distributions of the estimated overall survival (OS) for every group of clinicopathological characteristics.

Variables	*N*	Mean OS (months)	*P*
Sex			0.176
Male	52	81	
Female	30	95	
Age (years)			0.120
<60	59	90	
≥60	23	76	
Tumor size			0.281
≤7	71	89	
>7	11	72	
Tumor location			0.305
Left	40	82	
Right	42	89	
ECOG standard			0.013*
0	62	90	
≥1	20	69	
Fuhrman's grade			0.066
High	12	91	
Intermediate	54	90	
Low	16	71	
Stage			0.03*
I–II	62	91	
III–IV	20	73	
Risk			0.000**
Low	39	97	
Intermediate	31	87	
High	12	51	
Neutrophil			0.116
Normal	70	89	
<LLN or >ULN	12	77	
Lymphocyte			0.219
Normal	77	88	
<LLN or >ULN	5	72	
Hemoglobin			0.136
Normal	72	89	
<LLN or >ULN	10	72	
Platelets			0.001**
Normal	71	91	
<LLN or >ULN	11	59	
Urea nitrogen			0.332
Normal	68	88	
>ULN	14	78	
LDH			0.017*
Normal	77	89	
<LLN or >ULN	5	58	
β2-MG			0.524
Normal	67	89	
>ULN	15	85	

ECOG, Eastern Cooperative ONcology Group; LDH, lactic dehydrogenase; LLN, lower limit of normal; ULN, upper limit of normal; β2-MG, beta-2 microglobulin; OS, overall survival. $^*P < 0.05$; $^{**}P < 0.01$.

TABLE 2 | Univariate analysis of 82 RCC patients on all biomarkers and overall survival.

Parameters	OS		
	Hazard ratio	95%CI	*P*
$PD\text{-}L1^{+}_{IM}$	1.001	0.999–1.002	0.454
$PD\text{-}L1^{+}_{CT}$	1.001	1.000–1.001	0.115*
$CD3^{+}_{IM}$	0.998	0.995–1.001	0.193*
$CD3^{+}_{CT}$	0.992	0.986–0.998	0.013**
$CD4^{+}_{IM}$	0.996	0.992–1.001	0.127*
$CD4^{+}_{CT}$	0.995	0.988–1.002	0.149*
$CD45RO^{+}_{IM}$	0.997	0.992–1.001	0.134*
$CD45RO^{+}_{CT}$	0.999	0.993–1.004	0.677
$Foxp3^{+}_{IM}$	1.000	0.999–1.002	0.684
$Foxp3^{+}_{CT}$	1.000	0.998–1.002	0.776
$CD4^{+}Foxp3^{+}_{IM}$	1.002	0.994–1.009	0.648
$CD4^{+}Foxp3^{+}_{CT}$	1.004	0.991–1.018	0.528
$CD4^{+}Foxp3^{+}CD45RO^{+}_{IM}$	0.993	0.970–1.017	0.591
$CD4^{+}Foxp3^{+}CD45RO^{+}_{CT}$	1.018	0.992–1.044	0.182*
$TNFR2^{+}_{IM}$	1.000	0.998–1.003	0.679
$TNFR2^{+}_{CT}$	1.001	1.000–1.002	0.104*
$CD4^{+}Foxp3^{+}TNFR2^{+}_{IM}$	1.004	0.995–1.013	0.365
$CD4^{+}Foxp3^{+}TNFR2^{+}_{CT}$	1.012	1.000–1.025	0.059*
$CD3^{+}PD\text{-}L1^{+}_{IM}$	0.988	0.977–0.999	0.039**
$CD3^{+}PD\text{-}L1^{+}_{CT}$	0.996	0.989–1.003	0.223
IDO^{+}_{IM}	1.001	0.999–1.004	0.331
IDO^{+}_{CT}	1.000	0.999–1.001	0.964
$PD\text{-}1^{+}_{IM}$	1.001	0.987–1.014	0.918
$PD\text{-}1^{+}_{CT}$	0.996	0.980–1.012	0.616
$CD68^{+}PD\text{-}1^{+}_{IM}$	1.026	0.992–1.061	0.140*
$CD68^{+}PD\text{-}1^{+}_{CT}$	0.852	0.623–1.166	0.318
$CD8^{+}PD\text{-}1^{+}_{IM}$	1.022	0.998–1.047	0.071*
$CD8^{+}PD\text{-}1^{+}_{CT}$	0.925	0.831–1.030	0.157*
CK^{+}_{IM}	1.000	0.998–1.001	0.624
CK^{+}_{CT}	0.930	0.998–1.002	0.930
$CD8^{+}_{IM}$	1.002	0.999–1.004	0.267
$CD8^{+}_{CT}$	0.998	0.994–1.002	0.316
$CD68^{+}_{IM}$	1.003	1.000–1.006	0.033**
$CD68^{+}_{CT}$	0.992	0.980–1.003	0.162*
$CD8^{+}IDO^{+}_{IM}$	1.015	0.988–1.042	0.288
$CD8^{+}IDO^{+}_{CT}$	0.995	0.976–1.014	0.604
$CD68^{+}IDO^{+}_{IM}$	1.002	0.951–1.055	0.947
$CD68^{+}IDO^{+}_{CT}$	0.989	0.944–1.036	0.989

*$P < 0.2$; **$P < 0.05$.

detected using a series of Opal fluorophores (Opal520, Opal 540, Opal 570, Opal620, or Opal690) in another six-color IHC.

Visualization of the seven-color Opal slides was performed using a Mantra Quantitative Pathology Imaging System (PerkinElmer), which captured the fluorescent spectra at 20-nm wavelength intervals from 420 to 720 nm with the same exposure times to produce combined single-stack images. Images of single-stained and unstained tissue were used to extract the spectrum of each fluorophore and of tissue autofluorescence, separately, and to create the spectrum required for multispectral unmixing, which was performed using InForm image analysis software (PerkinElmer).

Five representative fields were selected to scan the CT and IM, respectively. The density was recorded as the number of positive cells per unit tissue surface area at ×200 magnification (1 mm). The nucleated stained cells in each area were quantified and expressed as the number of cells per area.

Statistical Analysis

The OS was calculated from the time of surgery until death with patients still alive censored at the time of their last contact in January 2018. The binary variables were analyzed by the Kaplan-Meier method, while triad or continuous variables were assessed by the Cox approach. A Cox proportional hazards model was used in multivariable analyses using the Forward-LR method with a significance level of 0.20 for entering and removing variables, resulting in a three-feature-based model to assess the prognostic value. The correlations of cell densities with different biomarkers were evaluated by Spearman's correlation analysis to determine why some variables were included or removed from the model. Receiver operator characteristic (ROC) curve analysis was used to compare the neo-IS to the IS proposed by the SITC. $P < 0.05$ in two-sided tests indicated statistical significance. All calculations were performed using IBM SPSS Statistics for Windows, version 22.0.

RESULTS

Patient Characteristics and Neo-IS_{RCC} Construction

The detailed clinicopathological characteristics of the 82 RCC patients are shown in **Table 1**. We identified a dominant cluster in multiplex fluorescent IHC analysis including 15 features out of a total of 19 biomarkers in the CT and IM ($CD3^{+}_{CT}$, $CD3^{+}PD\text{-}L1^{+}_{IM}$, $CD68_{IM}$, $P < 0.05$) ($PD\text{-}L1_{CT}$, $CD3_{IM}$, $CD4_{IM}$, $CD4_{CT}$, $CD45RO_{IM}$, $CD4^{+}Foxp3^{+}CD45RO^{+}_{CT}$, $TNFR2_{CT}$, $CD4^{+}Foxp3^{+}TNFR2^{+}_{CT}$, $CD68^{+}PD\text{-}1^{+}_{IM}$, $CD8^{+}PD\text{-}1^{+}_{IM}$, $CD8^{+}PD\text{-}1^{+}_{CT}$, $CD68_{CT}$, $P < 0.2$) (**Table 2**). The multispectral images of each biomarker were recorded (**Figure 1**). The correlations with 15 features were analyzed by Spearman analysis, which resulted in some features being included and removed from the multivariable Cox regression. The $CD3^{+}_{CT}$ cell density was positively correlated to those of $CD3^{+}_{IM}$, $CD4^{+}_{IM}$, $CD4^{+}_{CT}$, and $CD3^{+}PD\text{-}L1^{+}_{IM}$ cells ($P < 0.01$) (**Figures 2A–D**). The $CD4^{+}Foxp3^{+}CD45RO^{+}_{CT}$ cell density was positively correlated to those of $PD\text{-}L1^{+}_{CT}$, $CD4^{+}Foxp3^{+}CD45RO^{+}_{IM}$, and $CD4^{+}Foxp3^{+}TNFR2^{+}_{CT}$ cells ($P < 0.01$) (**Figures 3A,B,D**). In addition, the $CD4^{+}Foxp3^{+}CD45RO^{+}_{IM}$ cell density was positively correlated to that of $CD45RO^{+}_{IM}$ cells ($P < 0.01$) (**Figure 3C**), while $CD4^{+}Foxp3^{+}TNFR2^{+}_{CT}$ cell density was positively correlated with that of $TNFR2^{+}_{CT}$ cells ($P < 0.01$) (**Figure 3E**). The $CD8^{+}PD\text{-}1^{+}_{IM}$ cell density was positively correlated to those of $CD68^{+}_{IM}$, $CD68^{+}_{CT}$, $CD68^{+}PD\text{-}1^{+}_{IM}$, and $CD8^{+}PD\text{-}1^{+}_{CT}$ cells ($P < 0.01$) (**Figures 4A–D**).

We used multivariable Cox regression analysis to construct the neo-IS based on the levels of three features, where neo-IS =-PI (Prognostic Index) = $0.021 \times CD3^{+}_{CT}$ density$-0.116 \times CD4^{+}Foxp3^{+}CD45RO^{+}_{CT}$ density$-0.038 \times CD8^{+}PD\text{-}1^{+}_{IM}$

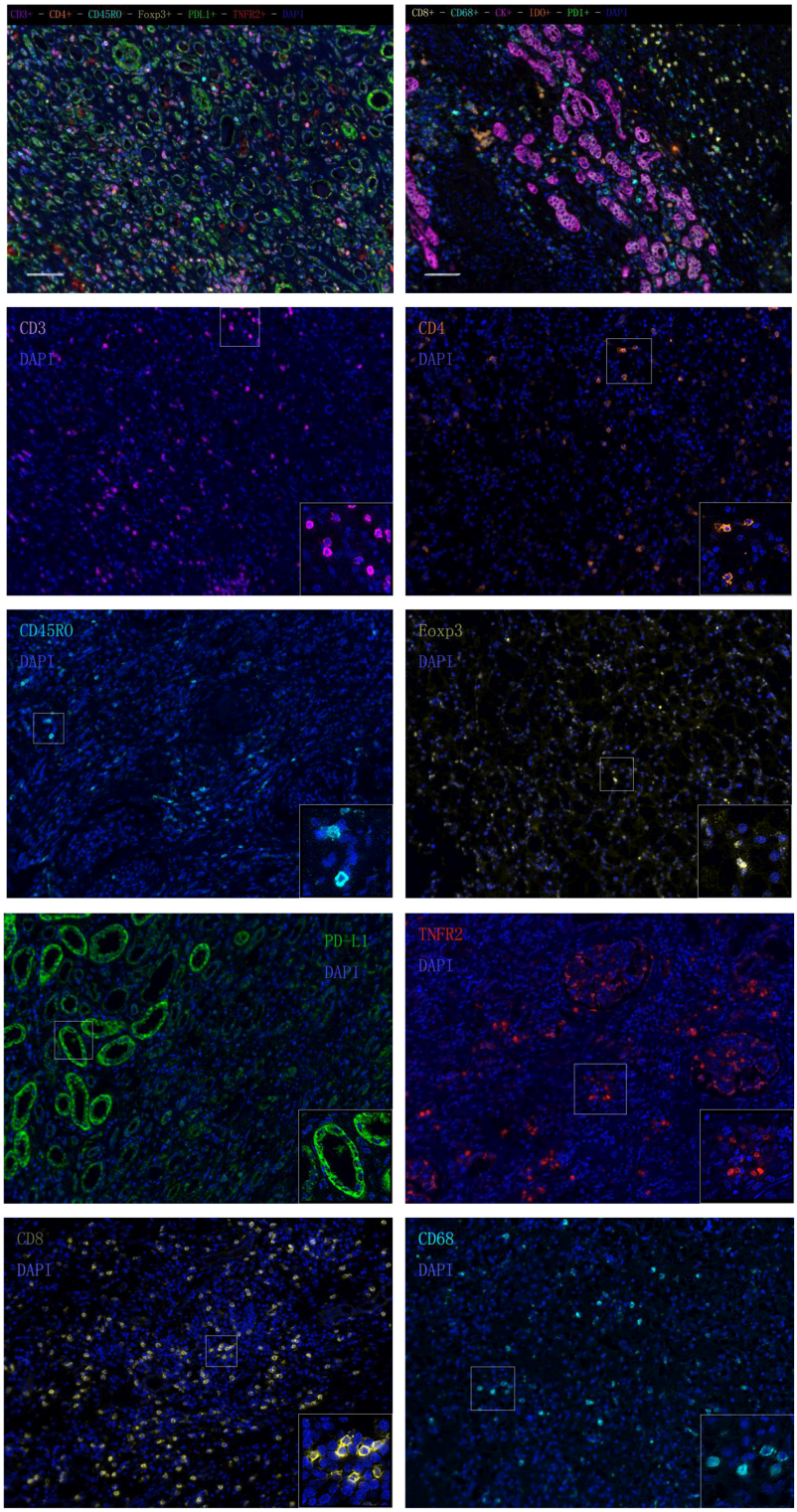

FIGURE 1 | Continued.

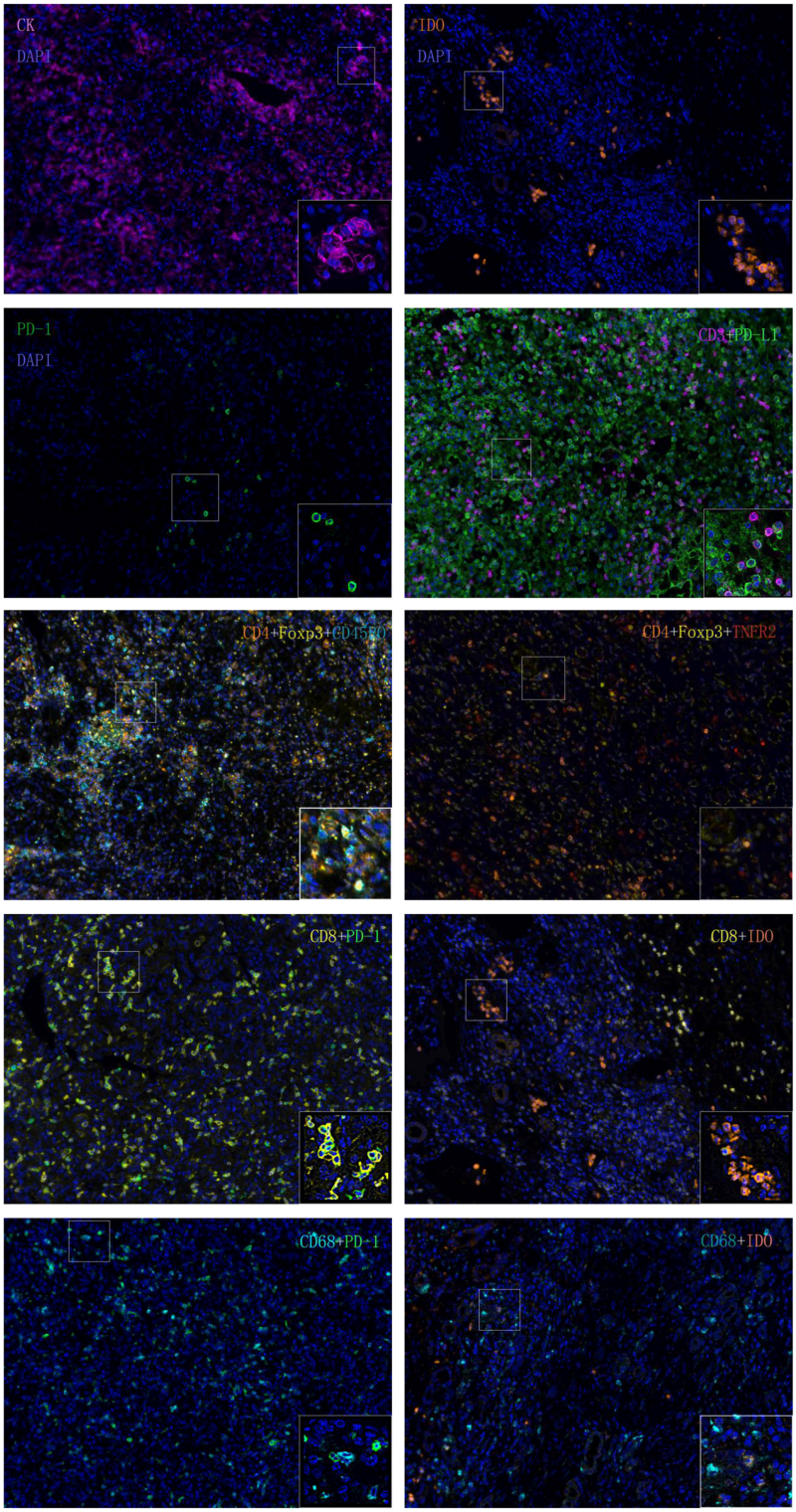

FIGURE 1 | Multiplex fluorescent immunohistochemistry staining.

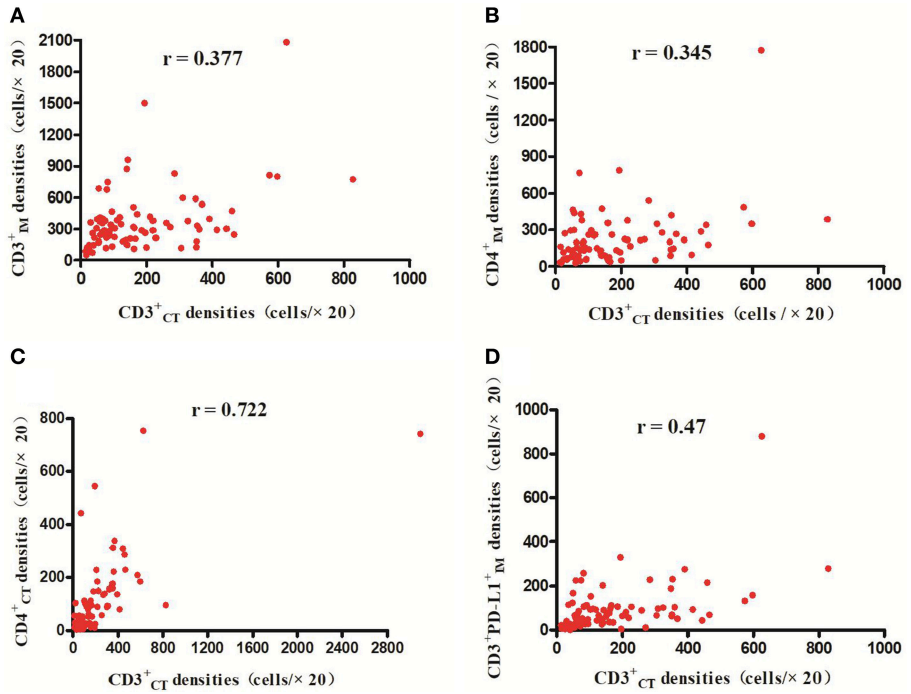

FIGURE 2 | Positive correlations between $CD3^{+}_{CT}$ and $CD3^{+}_{IM}$, $CD4^{+}_{IM}$, $CD4^{+}_{CT}$, and $CD3^{+}PD\text{-}L1^{+}_{IM}$ cell densities, respectively ($p < 0.01$) **(A–D)**.

density (**Figure 5**). The multivariable Cox model suggested that $CD3^{+}_{CT}$ cells played a protective role in the prognosis of RCC patients and that $CD4^{+}Foxp3^{+}CD45RO^{+}_{CT}$ T and $CD8^{+}PD\text{-}1^{+}_{IM}$ T cells were negative factors for the prognosis of RCC patients (**Table 3**).

Comparison of the IS Proposed by the SITC and the Neo-IS

The IS proposed by the SITC is based on the enumeration of two lymphocyte populations (CD3 or CD8) quantified within the CT and IM. It provides a scoring system ranging from IS 0 (I0), with low densities of both cell populations in both regions, to IS 4 (I4), with high densities of both cell types in both regions. Multivariable Cox regression survival analysis in the present study revealed that RCC patients with a higher IS proposed by the SITC had a better survival than that in those with lower IS (β −0.610, hazard ratio 0.543, 95%CI 0.343–0.860, $P < 0.01$). However, the AUC of the neo-IS was higher than that of the IS proposed by the SITC by ROC curve analysis (AUC 0.906 vs. 0.725, $P < 0.01$) (**Figure 6**).

Prognoses of RCC Patients With High and Low Neo-IS

The 3- and 5-year survival rates of the 82 RCC patients were 87.1 and 81.2%, respectively. The OS of these patients was 87 months (95% CI 80–94 months).

The 3- and 5-year survival rates in the neo-IS_{high} RCC patients were significantly higher than those in the neo-IS_{low} patients (94.7 vs. 77.4%, $P = 0.035$ and 94.7 vs. 64.5%, $P = 0.002$, respectively).

The OS in neo-IS_{low} patients was significantly shorter than that in neo-IS_{high} patients (73 vs. 97 months, $P = 0.000$) (**Figure 7**).

Prognoses of RCC Patients With Different Clinicopathological Characteristics

We compared the prognoses of 82 RCC patients according to sex, age, tumor size, tumor location, ECOG, histology, stage, risk stratification, *n*eutrophil, lymphocyte, LDH, hemoglobin, platelets, urea nitrogen, and β2-MG by univariate analysis (**Table 1**). The OS of patients with ECOG 0 was longer than that in those with ECOG ≥ 1 ($P = 0.013$) (**Figure 8A**). The OS of patients with stage I–II disease was longer than that in those with stage III–IV disease ($P = 0.030$) (**Figure 8B**). Patients with abnormal platelets had a significantly shorter OS than that in those with normal platelets ($P = 0.001$, **Figure 8C**). The diverse risk groups had significantly different OS ($P = 0.000$, **Figure 8D**). Patients with abnormal LDH had a significantly shorter OS than that in those with normal LDH ($P = 0.017$, **Figure 8E**). NLR had no prognostic value in patients with different NLR ($P = 0.324 > 0.05$).

Correlations Between Neo-IS and Clinicopathological Characteristics

There were no correlations between neo-IS and neutrophil ($P = 0.285 > 0.05$), lymphocyte ($P = 0.721 > 0.05$), platelets ($P = 0.132 > 0.05$), hemoglobin ($P = 0.054 > 0.05$), urea nitrogen

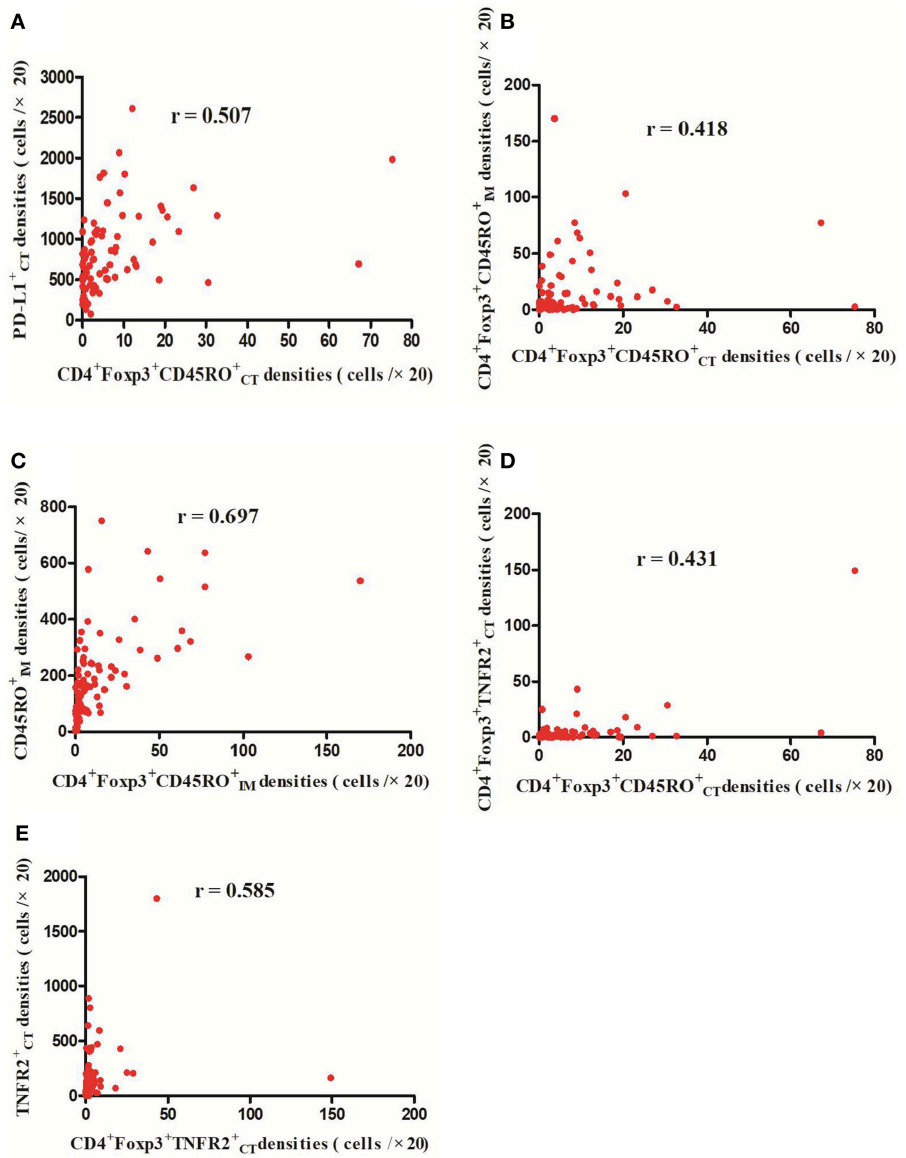

FIGURE 3 | Positive correlations between $CD4^+Foxp3^+CD45RO^+_{CT}$ and $PD\text{-}L1^+_{CT,}$ $CD4^+Foxp3^+CD45RO^+_{IM,}$ and $CD4^+Foxp3^+TNFR2^+_{CT}$ cell densities, respectively ($p < 0.01$) **(A,B,D)**; Meanwhile, $CD4^+Foxp3^+CD45RO^+_{IM}$ cell densities were positively related with $CD45RO^+_{IM}$ cell densities **(C)** ($p < 0.01$) and $CD4^+Foxp3^+TNFR2^+_{CT}$ cell densities were positively correlated with $TNFR2^+_{CT}$ cell densities ($p < 0.01$) **(E)**.

($P = 0.306 > 0.05$), β2-MG ($P = 0.150 > 0.05$), LDH ($P = 0.116 > 0.05$), or NLR ($P = 0.245 > 0.05$).

The neo-IS was also not related with Fuhrman's grade ($P = 0.111 > 0.05$), tumor size ($P = 0.626 > 0.05$), tumor location ($P = 0.716 > 0.05$) *or* risk stratification ($P = 0.087 > 0.05$). However, neo-IS was negatively correlated to staging ($r = -0.226$, $P = 0.041 < 0.05$) and ECOG ($r = -0.223$, $P = 0.044 < 0.05$).

Multiple-Factor Analysis of the Prognostic Factors in Patients With RCC

Multivariable Cox regression analysis revealed that risk stratification was a negative prognostic factor in RCC patients ($\beta = 2.422$, hazard ratio = 11.263, 95%CI: 1.610–78.82, $P = 0.015 < 0.05$) and that the neo-IS ($\beta = -0.810$, hazard ratio = 0.445, 95%CI: 0.284–0.696, $P = 0.000 < 0.01$) was a predictive factor in RCC patients.

There was no correlation between the neo-IS and risk stratification ($P = 0.087 > 0.05$). However, risk stratification was positively correlated to platelets ($r = 0.237$, $P < 0.05$), ECOG ($r = 0.281$, $P < 0.05$), and staging ($r = 0.573$, $P < 0.01$); thus, staging, ECOG, and platelets removed from the multivariable Cox regression.

The OS of neo-IS_{high} RCC patients with low- and intermediate- risk was longer than that of neo-IS_{low} patients ($P = 0.026$) ($P = 0.019$) (**Figures 9A,B**). With the limited cases

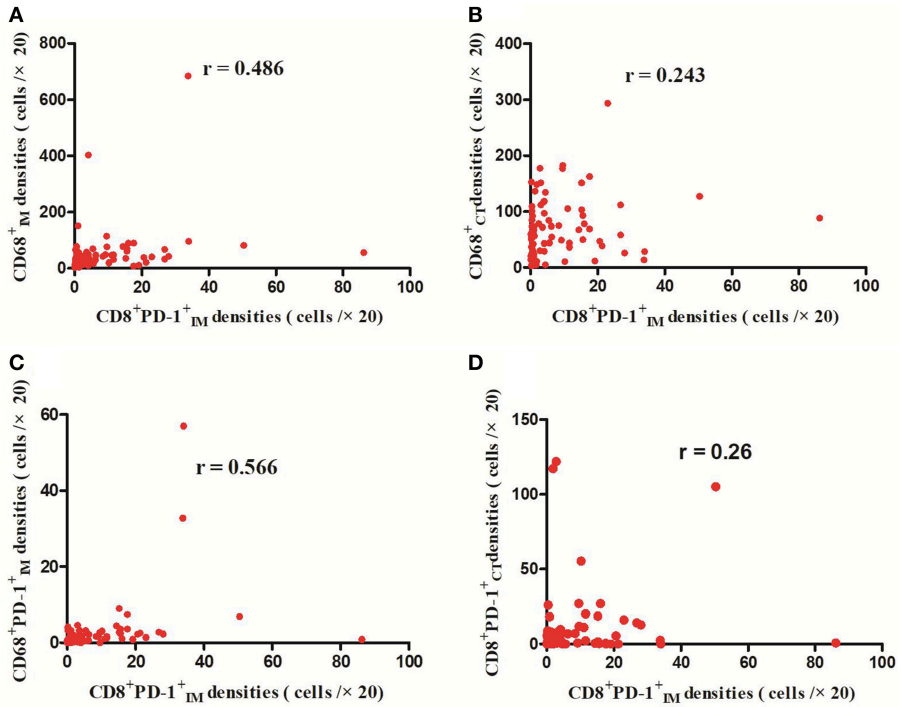

FIGURE 4 | Positive correlations between $CD8^+PD\text{-}1^+_{IM}$ and $CD68^+_{IM}$, $CD68^+_{CT}$, $CD68^+PD\text{-}1^+_{IM}$, and $CD8^+PD\text{-}1^+_{CT}$ cell densities ($p < 0.01$) **(A–D)**.

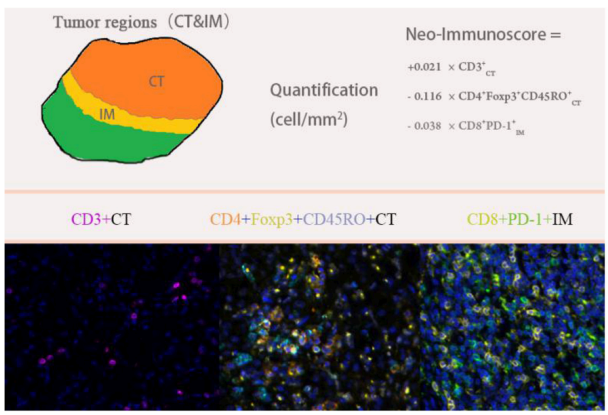

FIGURE 5 | Neo-Immunoscore definition and methodology.

of high-risk patients, we found that median survival time of six neo-IS_{high} RCC patients was longer than those of neo-IS_{low} patients (**Figure 10**).

DISCUSSION

Although developments in diagnostic imaging techniques have enabled the early detection of RCC, 20–30% of patients treated for localized RCC will experience tumor recurrence and metastasis after surgical resection (20). The high rates of

TABLE 3 | Multivariable analysis of 82 RCC patients on the selected biomarkers and overall survival.

Parameters	OS		
	Hazard ratio	95%CI	*P*
$CD3_{CT}$	0.979	0.969–0.990	0.000
$CD4^+Foxp3^+CD45RO^+_{CT}$	1.123	1.061–1.188	0.000
$CD8^+PD\text{-}1^+_{IM}$	1.039	1.004–1.074	0.027

tumor recurrence and metastasis emphasize the significance of postoperative surveillance. The nucleolar grading system and pTNM staging are prognostic factors validated by the International Society of Urological Pathology (ISUP) consensus (21). The various outcomes of RCC patients require an accurate prognostic model to guide the follow-up. These models are mostly composed of clinical factors and pathological features. The UISS, which divides localized RCC into three grades, is used frequently at present (4). Therefore, we analyzed the prognostic value of TNM staging, risk stratification, pathological features, and other clinical factors in RCC patients. We found that platelets, ECOG, staging, and risk stratification played roles in the prognosis of localized RCC patients in univariate analysis.

Although the TNM staging system, risk stratification, and other clinicopathological indicators were not considered with host immunity, increasing evidence suggests that an IS including CD3-positive and CD8-positive cell densities in TC and IM had a prognostic value to supplement the TNM staging system (7).

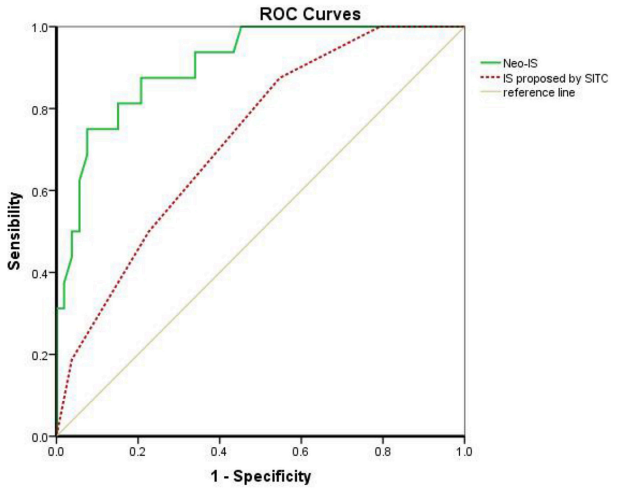

FIGURE 6 | Comparison of the IS proposed by the SITC and the neo-IS. IS proposed by SITC calculated with CD3 and CD8 by CT/ IM. Neo-IS = 0.021 × $CD3^{+}_{CT}$ density−0.116 × $CD4^{+}Foxp3^{+}CD45RO^{+}_{CT}$ density−0.038 × $CD8^{+}PD\text{-}1^{+}_{IM.}$ Density.

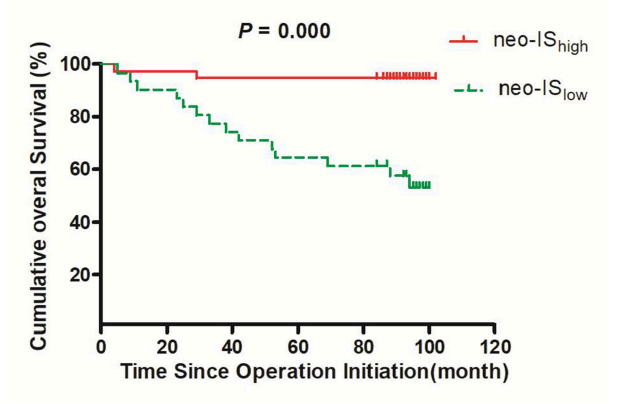

FIGURE 7 | Survival curves for overall survival (OS) in the neo-IS_{low} and neo-IS_{high} groups.

In order to promote the use of the IS proposed by the SITC in clinics, an international task was launched (22). In our study, RCC patients with a higher IS in that proposed by the SITC had a better survival compared with patients who had a lower IS. This finding is consistent with that of the prognostic value of the IS proposed by the SITC in gastrointestinal and other cancers.

The IS proposed by the SITC provides a score ranging from 0 (I0), with low CD3 and CD8 cell densities found in the CT and IM, to 4 (I4), with high densities of both cell types in both regions. Although the IS proposed by the SITC includes CD3 and CD8 in the CT and IM, the roles of different cell types in different regions are uncertain. So, we built a neo-IS based on densities of immune cells in the CT and IM, respectively.

The CD3 antigen is a pan-T cell marker which is expressed on all T cells and comprises the T cell receptor as a protein complex. The densities of $CD3^{+}$ tumor-infiltrating lymphocytes might reflect ongoing immunity against tumor cells and has been attributed to positive outcomes in breast cancers (23). Total T lymphocyte (CD3) densities in the CT were also significantly correlated with survival in colorectal cancer patients (24). We also found $CD3^{+}_{CT}$ T cells to be a protective factor in RCC patients (**Table 3**), which is consistent with the findings in other cancers. Immune checkpoints on infiltrating T cells are key regulators of immune escape in cancers. In recent years, studies on immune checkpoint molecules including PD-1/PD-L1 have attracted increasing attention. PD-1 is a member of B7 family that regulates T cell antigen-specific receptor signaling. PD-L1 binds to PD-1 to deliver an inhibitory signal to T cells and functions as a negative regulator of immunity. PD-L1 expressed on tumor cells or lymphocytes was associated with poor survival in RCC patients and PD-L1 expressed on activated T cells down-regulated primed T cells responses (25). However, we found that $CD3^{+}PD\text{-}L1^{+}_{IM}$ played a positive role (β −0.012, $P = 0.039$ $P < 0.05$) in univariate analysis but it was removed from the multivariate regression analysis for its correlation with $CD3^{+}_{CT}$. Our finding suggests that $CD3^{+}$ cells in the tumor microenvironment still affect important survival benefits despite partial disturbance of the anti-tumor immunity of $CD3^{+}$ cells by PD-L1 co-expression.

A number of studies have shown that increased CD8+ T cell infiltration was related to a good prognosis in many cancers (26); however, several exceptions have emerged in RCC. Primary studies on RCC showed that PD-1 expression on immune cells was associated with a poor clinical outcome (27) and infiltration of intratumoral PD-1+ T cells was an independent adverse predictor of survival (28), whereas our study observed that $CD8^{+}PD\text{-}1^{+}_{IM}$, which had a negative effect on survival in RCC, remained in the neo-IS due to its correlation with $CD8^{+}PD\text{-}1^{+}_{CT}$ (**Figure 4D**).Its role may be due to the inhibition of tumor immunity by $PD\text{-}1^{+}CD8^{+}_{IM}$ immune cells (29).

$CD68^{+}$ macrophages are innate immune cells that play a broad role in host defense and the maintenance of tissue homeostasis, but some research had shown that increased $CD68^{+}$ macrophage densities were related to increased tumor progression and worse prognosis in RCC patients (30). In univariate analysis, we also found that high $CD68^{+}_{IM}$ macrophage densities were a factor (β 0.003, $P = 0.033 < 0.05$) associated with the prognosis of RCC patients. This finding suggests that $CD68^{+}_{IM}$ macrophages may be favorable for the immunosuppressive M2 phenotype in RCC. However, $CD68^{+}_{IM}$ was removed from the neo-IS for its correlation with $PD\text{-}1^{+}CD8^{+}_{IM}$. IDO is an enzyme that catalyzes the degradation of the amino acid tryptophan and plays a critical role in immunosuppressive mechanisms. The expression and localization of IDO in the tumor microenvironment are diverse, including tumor cells and immune cells (31). However, one study reported IDO-1 expression to be totally absent in tumor cells and only present in a few macrophages, while its expression was positively correlated with CD8+ T cell expression (32). We used CK to label tumor epithelial cells. Similarly, we found no expression of $IDO^{+}CK^{+}$ cells in our study. Nevertheless, we found that the low co-expression of $IDO^{+}CD8^{+}$ or $IDO^{+}CD68^{+}$ in RCC had no predictive value for RCC prognosis.

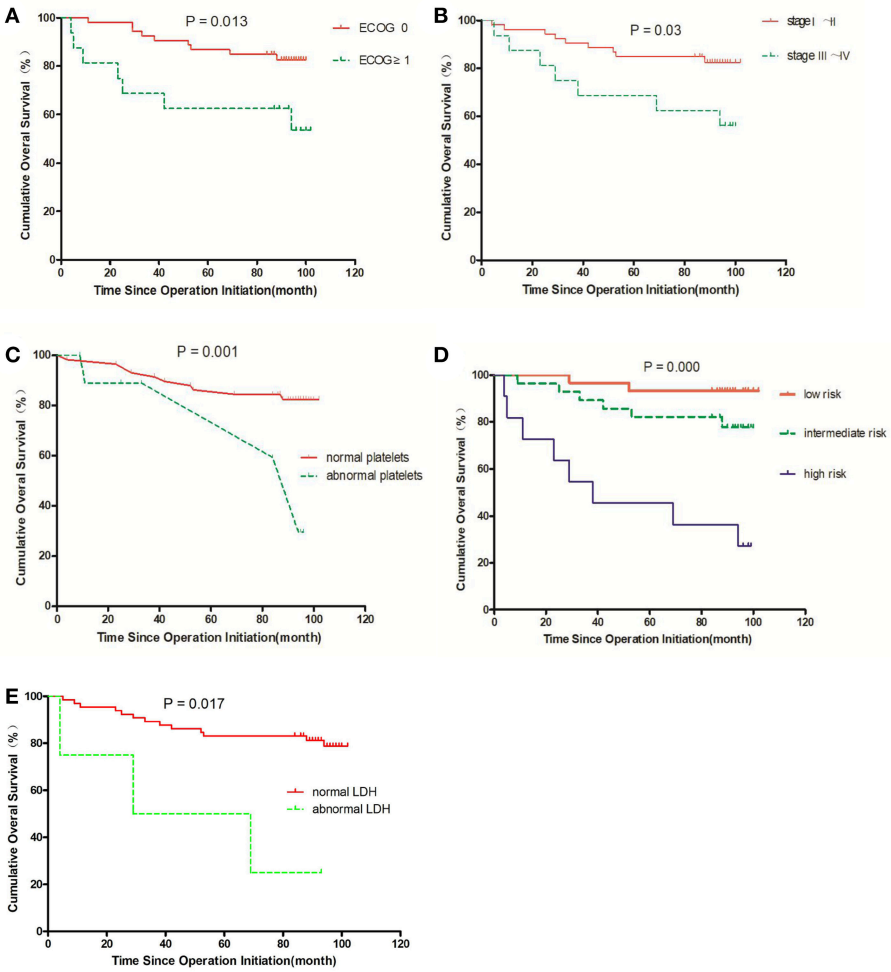

FIGURE 8 | Survival curves for overall survival (OS) in RCC patients; an event is defined as death from any cause in OS. The comparisons are as follows: **(A)** ECOG status; **(B)** stage; **(C)** normal or abnormal platelets; **(D)** risk group; **(E)** normal or abnormal LDH.

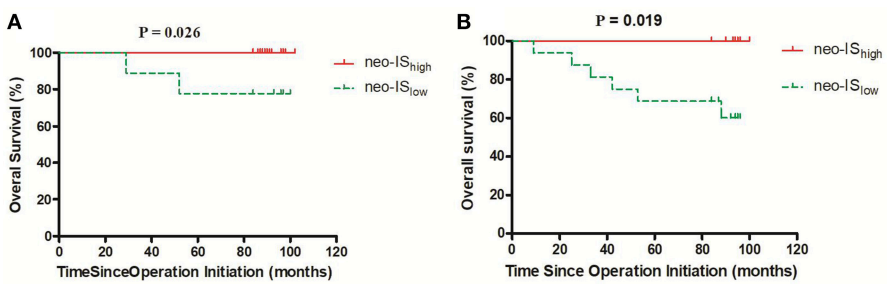

FIGURE 9 | Survival curves for overall survival (OS) in RCC patients with low- and intermediate-risk stratification. **(A)** Low-risk stratification. **(B)** Intermediate-risk stratification.

Treg, characterized by expression of the forkhead family transcription factor T Foxp3, are essential components of homeostasis in the immune system, which inhibits the functions of differentiated CD4+ and CD8+ T cells and activities of B cells, macrophages, and natural killer cells (33). High peritumoral levels of Tregs predicted deleterious outcomes in RCC, while Tregs in intratumoral areas had no prognostic value in RCC (34). However, in our study, $CD4^{+}Foxp3^{+}_{IM}$ and $CD4^{+}Foxp3^{+}_{CT}$ had no prognostic value in RCC. TNFR2 is a member of the TNFR family, also known as the TNFR

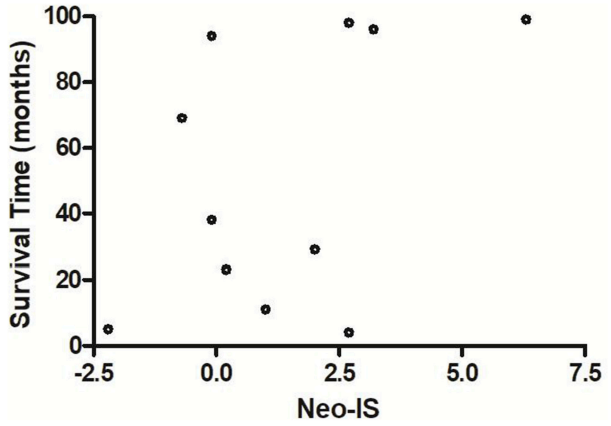

FIGURE 10 | Survival time of different neo-IS with high-risk RCC patients.

superfamily. TNFR2 has two types, membrane-binding TNFR2 (mTNFR2) and soluble TNFR2 (sTNFR2) (35). Treg cells expressing TNFR2 is the maximally suppressive subgroup of Treg in humans. $TNFR2^{+}$Treg contributed to cervical cancer development (36) but had no prognostic value in RCC in our study. In humans, $CD45RO^{+}$ are thought to be memory T cells. Memory T cells are generated during antigen-mediated immune responses and survive for a long time even in the absence of antigens in the peripheral tissues. Primary studies found that increasing infiltration of $CD45RO^{+}$ lymphocytes was correlated with increased survival in colorectal and gastric tumor immunity (37), but RCC patients with low $CD45RO^{+}$ T cell densities had a significantly better prognosis than that in patients with high densities (38). In our study, we also found no prognostic value for CD45RO in RCC. However, memory Treg (mTreg) cells, which reside in tissues after the elimination of antigens, have a high immunosuppressive capacity and decreased proliferative index (14, 39). The results of our study suggested that a high density of mTreg $(CD4^{+}Foxp3^{+}CD45RO^{+})_{CT}$ in RCC patients predicted a poor prognosis.

The neo-IS was constructed using three features; namely, CD3, $CD4^{+}Foxp3^{+}CD45RO^{+}$, and $CD8^{+}PD\text{-}1^{+}$ and included immunosuppression-related factors such as memory Treg cells and immune-checkpoint receptor positive CD8 T cells. The neo-IS not only included more biomarkers but also analyzed specific cell subsets by multiplex fluorescent IHC in the CT and IM, including $CD4^{+}Foxp3^{+}CD45RO^{+}$ in the CT and $CD8^{+}PD\text{-}1^{+}$ in the IM. We found that the AUC of the neo-IS was higher than that of the IS proposed by the SITC. Therefore, the neo-IS was more precise and comprehensive than the IS proposed by the SITC in our study.

Risk stratification and neo-IS were independent factors for the prognosis of RCC patients in our study. Moreover, a lower neo-IS suggested a worse outcome in RCC patients with low- and intermediate- risk stratification. Hence, the neo-IS may supplement the prognostic value of risk stratification to guide surveillance and subsequent therapy. It suggests that we should follow-up more frequently with $neo\text{-}IS_{low}$ RCC patients of low- and intermediate- risk than $neo\text{-}IS_{high}$ RCC patients *to* find the recurrence of patients earlier. Meanwhile, the neo-IS may be useful to guide further immunotherapy such as anti-PD-1 for recurrent patients. The present study of neo-IS was based on a relatively small cohort of 82 patients from a single center. A large-scale and multi-center perspective study is planned to further validate the neo-IS.

DATA AVAILABILITY

All datasets generated for this study are included in the manuscript and/or the supplementary files.

ETHICS STATEMENT

This research project was approved by the Ethics Committee of Tianjin Cancer Institute and Hospital. Written consents were obtained from each patient.

CONSENT FOR PUBLICATION

Written consents were obtained from each patient to publishing their pathological images as represent Figures.

AUTHOR CONTRIBUTIONS

CG, FW, and XR analyzed and interpreted the patient data. CG, HZ, and SB performed the multiplex fluorescent immunohistochemistry (IHC) staining and multispectral imaging of the cancer tissues. CG, YW, and ZY participated statistical analysis. CG was a major contributor in writing the manuscript. XR and FW interpreted and revised the manuscript. All authors read and approved the final manuscript.

FUNDING

National Key Research and Development Program (2018YFC1313400).

REFERENCES

1. Motzer Robert J, Jonasch E, Aqarwal N, Bhayani S, Bro WP, Chang SS, et al. Kidney cancer, version 2.2017, NCCN Clinical practice guidelines in oncology. *J Natl Compr Canc Netw.* (2017) 15:804–34. doi: 10.6004/jnccn.2017.0100
2. Fitzmaurice C, Dicker D, Pain A, Hamavid H, Moradi-Lakeh M, MacIntyre MF, et al. The global burden of cancer 2013. *JAMA Oncol.* (2015) 1:505–27. doi: 10.1001/jamaoncol.2015.0735
3. *Cancer Stat Facts: Kidney and Renal Pelvis Cancer.* Available online at: http://seer._cancer.gov/statfacts/html/kidrp._html (accessed December, 2018)

4. Escudier B, Porta C, Schmidinger M, Rioux-Leclercq N, Bex A, Khoo V, et al. Renal cell carcinoma: ESMO clinical practice guidelines for diagnosis, treatment and follow-up. *Ann Oncol.* (2016) 27:v58–68. doi: 10.1093/annonc/mdw328
5. Galon J, Fridman WH, Pages F. The adaptive immunologic microenvironment in colorectal cancer: a novel perspective. *Cancer Res.* (2007) 67:1883–6. doi: 10.1158/0008-5472.CAN-06-4806
6. Fridman WH, Pages F, Sautes-Fridman C, Galon J. The immune contexture in human tumours: impact on clinical outcome. *Nat Rev Cancer*. (2012) 1:298–306. doi: 10.1038/nrc3245
7. Galon J, Mlecnik B, Bindea G, Angell HK, Berger A, Lagorce C, et al. Towards the introduction of the 'Immunoscore' in the classifcation of malignant tumours. *J Pathol.* (2014) 232:199–209. doi: 10.1002/path.4287
8. Pages F, Mlecnik B, Marliot F, Bindea G, Ou FS, Bifulco C, et al. International validation of the consensus Immunoscore for the classification of colon cancer: a prognostic and accuracy study. *Lancet.* (2018) 391:2128–39. doi: 10.1016/S0140-6736(18)30789-X
9. Donnem T, Kilvaer TK, Andersen S, Richardsen E, Paulsen EE, Hald SM, et al. Strategies for clinical implementation of TNM-Immunoscore in resected nonsmall-cell lung cancer. *Ann Oncol.* (2016) 27:225–32. doi: 10.1093/annonc/mdv560
10. Zhang XM, Song LJ, Shen J, Yue H, Han YQ, Yang CL, et al. Prognostic and predictive values of immune infiltrate in patients with head and neck squamous cell carcinoma. *Hum Pathol.* (2018) 82:104–12. doi: 10.1016/j.humpath.2018.07.012
11. Sasidharan Nair V, Elkoed E. Immune checkpoint inhibitors in cancer therapy: a focus on T-regulatory cells. *Immunol Cell Biol*. (2018) 96:21–33. doi: 10.1111/imcb.1003
12. Jensen HK, Donskov F, Nordsmark M, Marcussen N, von der Maase H. Increased intratumoral FOXP3-positive regulatory immune cells during interleukin-2 treatment in metastatic renal cell carcinoma. *Clin Cancer Res.* (2009) 15:1052–8. doi: 10.1158/1078-0432.CCR-08-1296
13. Yan F, Du R, Wei F, Zhao H, Yu J, Wang C, et al. Expression of TNFR2 by regulatory T cells in peripheral blood is correlated with clinical pathology of lung cancer patients. *Cancer Immunol Immunother.* (2015) 64:1475–85. doi: 10.1007/s00262-015-1751-z
14. Rosenblum MD, Way SS, Abbas AK. Regulatory T cell memory. *Nat Rev Immuol.* (2016) 16:90–101. doi: 10.1038/nri.2015.1
15. Komohara Y, Hasita H, Ohnishi K, Fujiwara Y, Suzu S, Eto M, et al. Macrophage infiltration and its prognostic relevance in clear cell renal cell carcinoma. *Cancer Sci*. (2011) 102:1424–31. doi: 10.1111/j.1349-7006.2011.01945.x
16. Dermani FK, Samadi P, Rahmani G, Kohlan AK, Najafi R. PD-1/PD-L1 immune checkpoint: potential target for cancer therapy. *J Cell Physiol.* (2018) 234:1313–25. doi: 10.1002/jcp.27172
17. Liu H, Shen Z, Wang Z, Wang X, Zhang H, Qin J, et al. Increased expression of IDO associates with poor postoperative clinical outcome of patients with gastric adenocarcinoma. *Sci Rep.* (2016) 6:21319. doi: 10.1038/srep21319
18. Duan Q, Xu M, Zhang X, Jia M, Yuan R, Gan M. Clinical signifcance of cytokeratin in the cervical lymph nodes of patients with mandibular gingival squamous cell carcinoma. *Oncol Lett.* (2018) 16:3135–9. doi: 10.3892/ol.2018.9005
19. Mitchell TJ, Turajlic S, Rowan A, Nicol D, Farmery JHR, O'Brien T, et al. Timing the landmark events in the evolution of clear cell renal cell cancer: TRACERx renal. *Cell.* (2018) 173:611–23. doi: 10.1016/j.cell.2018.02.020
20. Williamson TJ, Pearson JR, Ischia J, Bolton DM, Lawrentschuk N. Guideline of guidelines: follow-up after nephrectomy for renal cell carcinoma. *BJU Int.* (2016) 117:555–62. doi: 10.1111/bju.13384
21. Delahunt B, Cheville JC, Martignoni G, Humphrey PA, Magi-Galluzzi C, McKenney J, et al. The International Society of Urological Pathology (ISUP) grading system for renal cell carcinoma and other prognostic parameters. *Am J Surg Pathol.* (2013) 37:1490–504. doi: 10.1097/PAS.0b013e318299f0fb
22. Galon J, Pages F, Marincola FM, Angell HK, Thurin M, Lugli A, et al. Cancer classification using the Immunoscore: a worldwide task force. *J Transl Med.* (2012) 10:205. doi: 10.1186/1479-5876-10-205
23. Rathore AS, Kumar S, Konwar R, Srivatava AN, Makker A, Goel MM. Presence of CD3+ tumor infiltrating lymphocytes is significantly associated with good prognosis in infiltrating ductal carcinoma of breast. *Indian J Cancer*. (2013) 50:239–44. doi: 10.4103/0019-509X.118744
24. Galon J, Costes A, Sanchez-Cabo F, Kiriovsky A, Mlecnik B, Lagorce-Pagès C, et al. Type, density, and location of immune cells within human colorectal tumors predict clinical outcome. *Science*. (2006) 313:1960–4. doi: 10.1126/science.1129139
25. Thompson RH, Gillett MD, Cheville JC, Lohse CM, Dong H, Webster WS, et al. Costimulatory B7-H1 in renal cell carcinoma patients: indicator of tumor aggressiveness and potential therapeutic target. *Proc Natl Acad Sci USA*. (2004) 101:17174–9. doi: 10.1073/pnas.0406351101
26. Becht E, Giraldo NA, Germain C, de Reyniès A, Laurent-Puig P, Zucman-Rossi J, et al. Immune contexture, immunoscore, and malignant cell molecular subgroups for prognostic and theranostic classifications of cancers. *Adv Immunol.* (2016) 130:95–190. doi: 10.1016/bs.ai.2015.12.002
27. Giraldo NA, Becht E, Pages F, Skliris G, Verkarre V, Vano Y, et al. Orchestration and prognostic significance of immune checkpoints in the microenvironment of primary and metastatic renal cell cancer. *Clin Cancer Res*. (2015) 21:3031–40. doi: 10.1158/1078-0432.CCR-14-2926
28. Thompson RH, Dong H, Lohse CM, Leibovich BC, Blute ML, Cheville JC, et al. PD-1is expressed by tumor-infiltrating immune cells and is associated with poor outcome for patients with renal cell carcinoma. *Clin Cancer Res.* (2007) 13:1757–61. doi: 10.1158/1078-0432.CCR-06-2599
29. Gordon SR, Maute RL, Dulken BW, Hutter G, George BM, McCracken MN, et al. PD-1 expression by tumour-associated macrophages inhibits phagocytosis and tumour immunity. *Nature*. (2017) 545:495–9. doi: 10.1038/nature22396
30. Kovaleva OV, Samoilova DV, Shitova MS, Gratchev A. Tumor associated macrophages in kidney cancer. *Anal Cell Pathol.* (2016) 2016: 9307549. doi: 10.1155/2016/9307549
31. Chen W. IDO: more than an enzyme. *Nat Immunol*. (2011) 12:809–11. doi: 10.1038/ni.2088
32. Seeber A, Klinglmair G, Fritz J, Steinkohl F, Zimmer KC, Aigner F, et al. High IDO-1 expression in tumor endothelial cells is associated with response to immunotherapy in metastatic renal cell carcinoma. *Cancer Sci.* (2018) 109:1583–91. doi: 10.1111/cas.13560
33. Sakaguchi S, Yamahuchi T, Nomura T, Ono M**.** Regulatory T cells and immune tolerance. *Cell.* (2008) 133:775–87. doi: 10.1016/j.cell.2008.05.009
34. Siddiqui SA, Frigola X, Bonne-Annee S, Mercader M, Kuntz SM, Krambeck AE, et al. Tumor-infiltration Foxp3-CD4+CD25+ T cells predict poor survival in renal cell carcinoma. *Clin Cancer Res*. (2007) 13:2075–81. doi: 10.1158/1078-0432.CCR-06-2139
35. Liu Z, Ma C, Ma G, Sun X, Liu J, Li S, et al. High expression of tumor necrosis factor receptor 2 in tissue is associated with progression and prognosis of esophageal squamous cell carcinoma. *Hum Pathol*. (2018) 80:179–85. doi: 10.1016/j.humpath.2018.03.027
36. Zhang T, Jiao J, Jiao X, Zhao L, Tian X, Zhang Q, et al. Aberrant frequency of $TNFR2^{+}$ Treg and related cytokines in patients with CIN and cervical cancer. *Oncotarget*. (2017) 9:5073–83. doi: 10.18632/oncotarget.23581
37. Lee HE, Chae SW, Lee YJ, Kim MA, Lee HS, Lee BL, et al. Prognostic implications of type and density of tumour-infiltrating lymphocytes in gastric cancer. *Br J Cancer.* (2008) 99:1704–11. doi: 10.1038/sj.bjc.6604738
38. Hotta K, Sho M, Fujimoto K, Shimada K, Yamato I, Anai S, et al. Prognostic significance of CD45RO+ memory T cells in renal cell carcinoma. *Br J Cancer*. (2011) 105:1191–6. doi: 10.1038/bjc.2011.368
39. Grata IK, Campbell DJ. Organ-specific and memory Treg cells: specificity, development, function, and maintenance. *Front Immunol.* (2014) 5:333. doi: 10.3389/fimmu.2014.00333

Conflict of Interest Statement: The authors declare that the research was conducted in the absence of any commercial or financial relationships that could be construed as a potential conflict of interest.